Broadband Printed Antennas for Waveguide-Based Spatial Power Combiners

Alexander B. Yakovlev[1*], Milan V. Lukich[1], Atef Z. Elsherbeni[1], Charles E. Smith[1], and Michael B. Steer[2]

[1]Department of Electrical Engineering, The University of Mississippi, University, MS 38677-1848

[2]Department of Electrical and Computer Engineering, North Carolina State University, Raleigh, NC 27695-7914

Abstract

In this paper we present a spatial power combining architecture consisting of several interacting printed antenna arrays placed at dielectric interfaces in multilayered waveguide. Narrowband resonant patch and slot antennas used in earlier designs are replaced by tapered meander line antennas and their modifications, in order to increase the frequency bandwidth and efficiency of the system and provide operation in multiple band regimes. The full-wave analysis of the interacting antenna modules presented here is based on the integral equation formulation for induced electric and magnetic surface current density discretized via the method of moments. Magnetic potential dyadic Green's functions are obtained for a multilayered rectangular waveguide.

I. Introduction

To exploit the advantages of solid-state technology for high power levels at microwave and millimeter-wave frequencies, the power from many individual devices must be combined because of the fundamental power-handling limitations of semiconductor devices at these frequencies. Alternatively, if power combining is achieved using waveguides and printed-circuit transmission lines, there is an upper limit on the number of components used due to losses in these waveguiding structures. Spatial power combining techniques provide high combining efficiency for high power levels in microwave and millimeter-wave regimes using free space rather than waveguide and transmission line junctions utilized in circuit-combining structures.

In this paper we present a spatial power combining architecture consisting of several interacting printed antenna arrays placed at dielectric interfaces in multilayered waveguide fed by a horn antenna (Fig. 1). In earlier designs we have used narrowband resonant patch and slot antennas [1], [2]. In the present study these are replaced by tapered meander line [3], microstrip loop, U-slot patch antennas, and their modifications, achieving increased frequency bandwidth, higher system efficiency, and providing operation in multiple band regimes. Signals collected by antenna arrays are coupled to the amplifier array through a ground plane containing meander line antennas and the amplified signal is then reradiated into free space through meander lines of another ground plane. Depending on the application, the amplified power can be radiated into free space [4] or collected by a receive horn [2]. Numerical results are presented for interacting meander line and patch antennas illustrating the advantages of their utilization in the waveguide-based power combining system.

II. Formulation and Green's Dyadics for Layered Waveguides

The entire amplifier system is modeled using a generalized scattering matrix approach by decomposing the system into smaller modules. Each module is characterized by a generalized scattering matrix (GSM), and the overall response of the system is obtained by cascading the GSMs of individual modules. To obtain the GSM for a multilayered waveguide containing electric and magnetic type antennas, a method of moments integral equation formulation is utilized for the discretization of electric and magnetic surface current densities. A coupled set of

0-7803-7330-8/02 $17.00 © 2002 IEEE

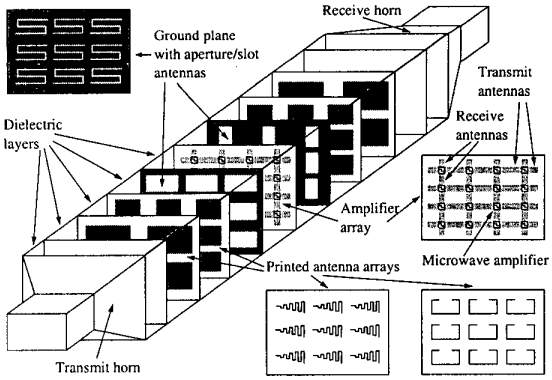

Fig. 1. Waveguide-based spatial power combining architecture.

integral equations is obtained by enforcing a boundary condition for the tangential components of the electric field on the metal surface of printed antennas and a continuity condition for the tangential components of the magnetic field across the surface of magnetic-type antennas in a ground plane (similar formulations have been implemented in [1], [2]).

In this formulation, magnetic potential dyadic Green's functions due to an arbitrarily oriented point source in a multilayered rectangular waveguide (Fig. 2) are obtained as the solution of the system of dyadic Helmholtz equations,

$$\nabla^2\overline{\overline{\mathbf{G}}}_{is}(\vec{r},\vec{r}') + k_i^2\overline{\overline{\mathbf{G}}}_{is}(\vec{r},\vec{r}') = -\delta_{is}\bar{\bar{\mathbf{I}}}\delta(\vec{r}-\vec{r}')\,, \qquad \vec{r}\in V_i, \quad \vec{r}'\in V_s \tag{1}$$

subject to the boundary conditions on the metal surface of waveguide (including a ground plane) S_M,

$$\hat{n}\times\overline{\overline{\mathbf{G}}}_{is}(\vec{r},\vec{r}') = 0, \quad \nabla\cdot\overline{\overline{\mathbf{G}}}_{is}(\vec{r},\vec{r}') = 0, \quad \vec{r}\in S_M \tag{2}$$

and mixed continuity conditions across dielectric interfaces S_i, $i = 1,2,...,N-1$,

$$\begin{aligned}
\hat{z}\times\overline{\overline{\mathbf{G}}}_{is}(\vec{r},\vec{r}') &= \hat{z}\times\overline{\overline{\mathbf{G}}}_{i+1s}(\vec{r},\vec{r}'), \qquad \vec{r}\in S_i\\
\hat{z}\cdot\overline{\overline{\mathbf{G}}}_{is}(\vec{r},\vec{r}') &= \hat{z}\cdot\overline{\overline{\mathbf{G}}}_{i+1s}(\vec{r},\vec{r}'), \qquad \vec{r}\in S_i\\
\hat{z}\times\nabla\times\overline{\overline{\mathbf{G}}}_{is}(\vec{r},\vec{r}') &= \hat{z}\times\nabla\times\overline{\overline{\mathbf{G}}}_{i+1s}(\vec{r},\vec{r}'), \qquad \vec{r}\in S_i\\
\frac{1}{\epsilon_i}\nabla\cdot\overline{\overline{\mathbf{G}}}_{is}(\vec{r},\vec{r}') &= \frac{1}{\epsilon_{i+1}}\nabla\cdot\overline{\overline{\mathbf{G}}}_{i+1s}(\vec{r},\vec{r}'), \qquad \vec{r}\in S_i.
\end{aligned} \tag{3}$$

Here, i and s correspond to field and source points, respectively, positioned in the regions V_i and V_s; δ_{is} is the Kronecker delta; $\hat{n}$ is an outward normal to the waveguide metal surface. The solution of the boundary value problem (1)-(3) is obtained in the form of a partial eigenfunction expansion over the complete system of orthonormal eigenfunctions of the Laplacian operator:

$$G_{is}^{\alpha\beta}(x,y,z,x',y',z') = \sum_{m=0}^{\infty}\sum_{n=0}^{\infty}\phi_{mn}^{\alpha}(x,y)\phi_{mn}^{\beta}(x',y')f_{mn}^{(is)\alpha\beta}(z,z'), \quad \alpha,\beta = x,y,z.$$

The one-dimensional characteristic Green's functions $f_{mn}^{(is)\alpha\beta}(z,z')$ are obtained in a closed form as a superposition of forward and backward traveling waves

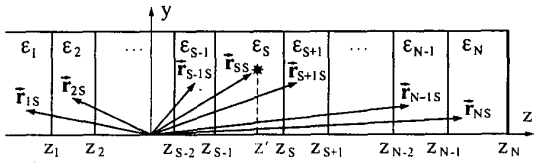

Fig. 2. Geometry of a multilayered rectangular waveguide associated with a Green's function problem.

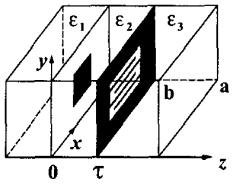

Fig. 3. Geometry of interacting patch and meander line antennas.

subject to the appropriate boundary and continuity conditions. The analytical form of Green's functions provides physical insight into resonance and surface wave effects occurring in overmoded layered waveguides.

III. Numerical Results and Discussions

Numerical results for the S-parameters of the interacting meander line and patch antennas (geometry shown in Fig. 3) in a rectangular waveguide transition operating at X-band are shown in Figs. 4 and 5. The results are obtained for the following geometrical and material parameters: the rectangular waveguide is 22.86 mm × 10.16 mm, slot length in a meander line is 11 mm, slot width is 0.5 mm, slot separation is 1 mm, a metal patch is 2 mm × 2 mm, $\epsilon_1 = \epsilon_3 = 1$, $\epsilon_2 = 3$. It can be seen (Figs. 4 and 5) that the use of meander line antenna in resonant antenna modules results in a significant increase of the bandwidth maintaining the low return loss at the resonant frequency. In particular, a five-slot meander line antenna produces approximately 20% bandwidth at –10 dB (dash-dotted line in Fig. 4) in comparison to the bandwidth of the single slot which is less than 5%. Also, it was observed that by increasing a separation between slots in a meander line, a wider bandwidth can be achieved (Fig. 6; solid and dash-dotted curves for comparison). In conclusion, the use of meander line antennas and their modifications in waveguide-based transitions shows significant advantages in scattering characteristics in comparison with the previously used rectangular patch and slot antennas.

References

[1] A. B. Yakovlev, A. I. Khalil, C. W. Hicks, A. Mortazawi, and M. B. Steer, "The generalized scattering matrix of closely spaced strip and slot layers in waveguide," *IEEE Trans. Microwave Theory Tech.*, Vol. 48, pp. 126-137, Jan. 2000.

[2] A. B. Yakovlev, S. Ortiz, M. Ozkar, A. Mortazawi, and M. B. Steer, "A Waveguide-based aperture-coupled patch amplifier array –- Full-wave system analysis and experimental validation," *IEEE Trans. Microwave Theory Tech.*, Vol. 48, pp. 2692–2699, Dec. 2000.

[3] C. P. Huang, A. Z. Elsherbeni, and C. E. Smith, "Analysis and design of tapered meander line antennas for mobile communications," *The Applied Computational Electromagnetics Society (ACES) Journal*, Vol. 15, No. 3, pp. 159–166, 2000.

[4] S. Ortiz, M. Ozkar, A.B. Yakovlev, M.B. Steer, and A. Mortazawi, "Fault tolerance analysis and measurement of a spatial power amplifier," *IEEE Int. Microwave Symp. Dig.*, pp. 1827–1830, May 2001.

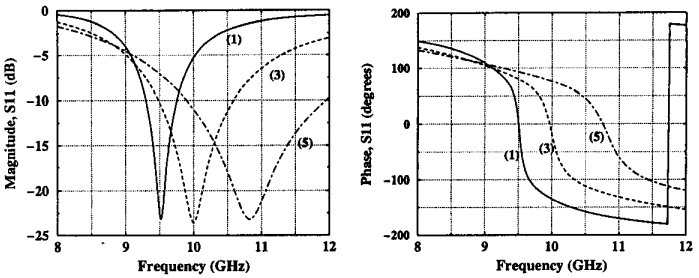

(a) (b)

Fig. 4. Magnitude (a) and phase (b) of the reflection coefficient S_{11} against frequency for the interacting meander line and patch antennas. A solid line is for the single slot (1), a dashed line is for the three-slot meander line (3), and a dash-dotted line is for the five-slot meander line (5).

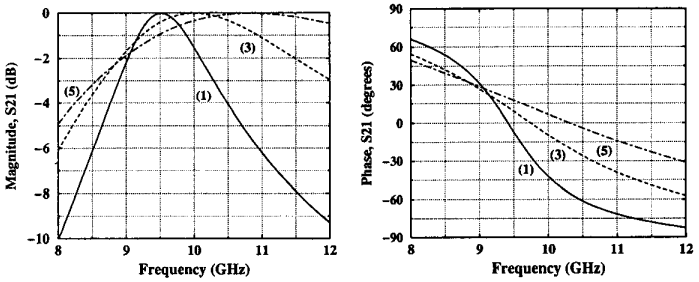

(a) (b)

Fig. 5. Magnitude (a) and phase (b) of the transmission coefficient S_{21} against frequency for the interacting meander line and patch antennas.

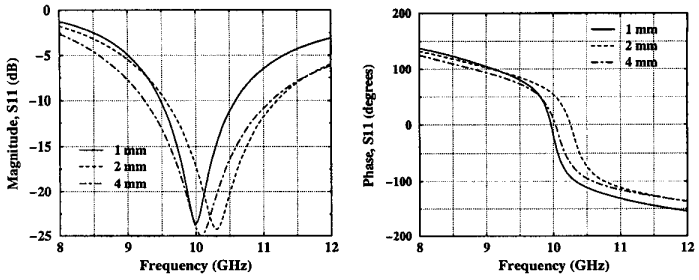

(a) (b)

Fig. 6. Magnitude (a) and phase (b) of the reflection coefficient S_{11} against frequency for different slot separation in the meander line coupled to a patch antenna.